

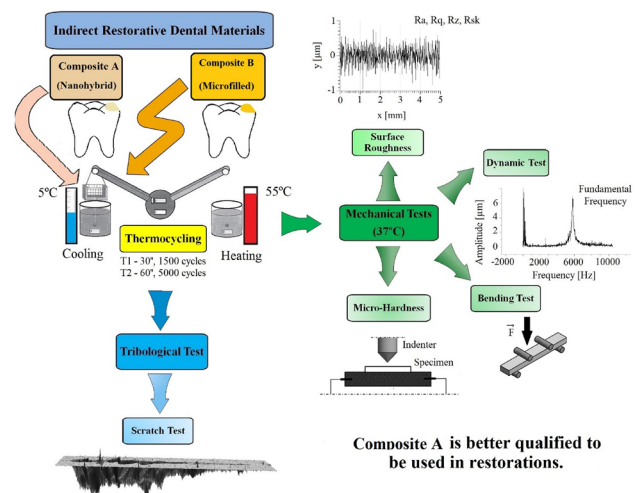
Thermocycling effect on mechanical and tribological characterization of two indirect dental restorative materials

M. Carreira¹ · P. V. Antunes¹ · A. Ramalho¹ · A. Paula² · E. Carrilho²

Received: 17 September 2015 / Accepted: 24 May 2016 / Published online: 15 June 2016
© The Brazilian Society of Mechanical Sciences and Engineering 2016

Abstract The purpose of this study is to evaluate the effects of aging by thermocycling on the mechanical and tribological properties of two indirect filling commercial resin-based restorative composite materials. The studied composites are referenced by the capital letters: A and B. The commercial trade names are omitted, to avoid commercial references. Forty specimens of each material were produced and divided into three groups: a control group not subjected to aging, and two groups, T₁ and T₂ submitted to different thermocycling conditions. The studied properties were surface roughness, elastic modulus (determined dynamically by impulse excitation of vibration, and statically by four-point bending test), flexural strength and work of fracture (four-point bending test), micro-hardness (Vickers micro-indentation) and coefficient of friction (scratch test). From this study, it was possible to conclude that Composite A, in addition to having better mechanical properties, is less affected by thermocycling than Composite B, which suggests that it will better withstand the stresses, both mechanical and thermal, which it is subjected to. It is also possible to infer that the thermocycling regimen proposed by Standard ISO 11405 (Dental materials—testing of adhesion to tooth structure, 2003) is not sufficient to adequately simulate the degradation caused by the oral

environment on current commercial resin-based restorative composites.



Graphical abstract

Keywords Resin composite · Thermocycling · Hardness · Flexural strength · Elastic modulus · Scratch test

1 Introduction

Currently, composite materials play a key role in biomedical applications, the aerospace industry, automobile industry and other engineering applications, as they exhibit outstanding performance [2].

The first commercial composites for dental restoration appeared in the 1960s and since then a lot of research has been carried out to improve their physical properties [2–8]. This development led to a wide range of commercial

Technical Editor: Estevam Las Casas.

✉ P. V. Antunes
pedro.antunes@dem.uc.pt

¹ CEMUC, Mechanical Engineering Department, University of Coimbra, Coimbra, Portugal

² Faculty of Medicine, University of Coimbra, Coimbra, Portugal

composite materials with different physical properties. Since improving one property may worsen another, it is essential to assess which properties should be improved, in order to produce composites that will better resist the mechanical, thermal and chemical stresses that dental restorative materials are subjected to in the oral cavity. Although the most accurate way to understand which commercial composites better withstand the oral environment would be through *in vivo* tests, their inherent difficulties do not allow this to be practical, making *in vitro* tests much more appealing.

Many papers about the influence of filler particles and different monomer combinations on the mechanical and tribological properties of resin composites have been published. Different monomer combinations have been tested to understand their influence on the mechanical properties of composites [3], to reduce the shrinkage that occurs during polymerization [4–6] and the water sorption in aqueous environments [7, 8]. The most frequently used monomers that constitute the resin matrix are bisphenol A-glycidyl methacrylate (Bis-GMA), triethylene glycol dimethacrylate (TEGDMA) and urethane dimethacrylate (UDMA). Modern composites have a wide range of filler particles, with different sizes, types, shapes and volume fractions, which will ultimately influence their physical properties. Resin composites are viscoelastic materials and, as such, their physical properties are highly dependent on several parameters, of which the most important are the oral temperature and the deformation rate [9]. Several studies demonstrate the importance of temperature in the physical properties of resin composites [9–12]. Ramalho et al. [10] studied the effect of temperature on the elastic modulus, flexural strength, toughness, micro-hardness and wear resistance of three direct posterior restoration resin composites and observed that all the above properties are very sensitive to temperature. Musanje and Darvell [11] state that properties obtained at temperatures other than 37 °C are inaccurate and do not adequately describe the behavior of these materials in the mouth. However, most studies found in the literature were done at room temperature and only rarely at nominal body temperature, 37 °C.

To simulate the effect that the oral environment has on restorative materials, aging techniques were developed. One of the most widely used techniques is thermocycling, which consists of subjecting the restorative materials to cyclic thermal stresses. The specimens are heated and cooled in baths, generally using distilled water, at the extreme temperatures that restorative materials are exposed to in the mouth. The material has a tendency to expand during heating and shrink during cooling. The difference between the coefficients of thermal expansion of

the organic resin matrix and the inorganic filler particles induces high mechanical stresses in the matrix/filler interface [13], promoting micro-leakage and fatigue fractures [14].

Gale and Darvell [12] analyzed 130 papers where thermocycling was used. Morresi et al. [15] examined 193 papers, published between 1998 and August of 2013, where thermocycling was used. Thermocycling is a controversial process because the results vary widely, which can be explained by the different bath temperatures, dwell times and number of cycles used by each researcher [12, 15].

The standard ISO 11405 [1] recommends that 500 thermal cycles be made, in baths at the extreme temperatures of 5 and 55 °C, with a dwell time of 20 s. However, such a regimen might not be enough to fully simulate the degradation caused by the oral environment on the restorative materials, which led several researchers to increase the number of thermal cycles, the bath temperatures and/or the dwell time of the specimens in the baths. Gale and Darvell [12] and Morresi et al. [15] observed that most researchers choose their own parameters, instead of following the regimen proposed by standard ISO 11405 [1].

Besides the evaluation of mechanical properties, the influence of thermocycling on the wear resistance is of vital importance. There is an expanding literature interest on a simple, yet refreshing and exciting test which adds understanding to wear damage processes, the scratch test. On the topic of the scratching and nanoscratching, Zheng et al. [16] investigated the microtribological behavior of human tooth using this technic. In recent literature, there are also some authors which use this technique to determine polymers and dental composites wear damage processes [17, 18].

Current dental composites have adequate mechanical properties for use in all areas of the mouth. But concern still exists when the materials are placed in high stress situations, especially in patients with bruxing or parafunctional habits. The concern here is for fracture of the restoration as well as wear. Wear is considered to be a lesser problem for current materials as compared to those that were the standard of care a decade ago, in large part due to refinement in the size of the reinforcing fillers which significantly reduced the magnitude of abrasive wear.

Due to the lack of specific international standards for restorative dental materials, to assess the more important properties it is essential to establish which properties are fundamental for direct restorative materials. The desired mechanical and physical properties are difficult to define because there is currently little correlation between the properties of composites and their clinical performance, resulting in difficulty to translate the *in vitro* results to *in vivo* ones.

Table 1 Resin composite materials under study and their composition, according to the manufacturers

Designation	Matrix	Reinforcement filler		
		Type	Dimension (μm)	Vol./weight (%)
Composite A	BisGMA, BisEMA, TEGDMA	Glass–ceramic particles, nano-particles of SiO_2	Micro-particles (1 μm) Nano-particles (20–40 nm)	73/89
Composite B	UDMA, aliphatic dimethacrylate	Nano-particles of SiO_2 , copolymer	Nano-particles (10–50 nm) Copolymer (–)	^a

BisGMA bisphenol A-glycidyl methacrylate, *BisEMA* ethoxylated bisphenol-A dimethacrylate, *TEGDMA* triethylene glycol dimethacrylate, *UDMA* urethane dimethacrylate

^a Composite B is a heterogeneous microfilled composite. The main reinforcement filler (62.9 % in weight) is a copolymer which consists of pre-polymerized ground up UDMA matrix and inorganic microfiller particles. Besides the copolymer, Composite B also contains highly dispersed silica particles (19.8 %)

Stress is a critical parameter for the success or failure of the adhesive interface and may lead to marginal gap formation. Elastic modulus obtained in vitro conditions, at ambient temperature and in dry conditions, does not have the same value when the material is applied in the mouth, hydration and temperature conditions will change and along with aging would affect the visco-elastic behavior of the composite material [19]. Contraction stress build-up occurs since shrinkage is obstructed and the material is rigid enough to resist sufficient plastic flow to compensate for the original volume [20].

The overall properties of a composite are influenced by the type, size, and volume fraction of the filler particles and the degree to which the filler is bonded to the resin matrix [21]. The type of matrix and the degree to which conversion occurs during polymerization also influence the properties, especially when aging occurs in the oral environment [21]. The presence of filler particles increases the compressive strength and hardness of the polymer matrix. Yang et al. [22] reported that changing the level of filler in composite altered the properties of hardness, water sorption, compressive strength, elastic modulus, and wear resistance [23].

Therefore, it is important to compare restorative composites to allow for the correct selection for each application needed, as this is essential to know the physical/tribological properties of dental composites relatively to other dental restorative materials.

In this work, two restorative resin commercial composites, available on the market, produced by different manufacturers and with distinct compositions, were subjected to aging by thermocycling. The aim of this study is to understand, according to their mechanical and tribological properties, which of the composites better withstands the degradation caused by thermocycling and which is better qualified to be used in posterior restorations, where they are exposed to high mechanical stresses during mastication.

2 Experimental work

The tests undertaken in the evaluation of the mechanical properties were: surface profilometry, impulse excitation of vibration, four-point bending and Vickers micro-hardness, which allow us to obtain the following properties: surface roughness, dynamic and static elastic modulus, flexural strength, work-of-fracture (WOF) and micro-hardness. The mechanical tests were done at a controlled temperature, to correctly evaluate how these materials behave at the nominal temperature of the oral cavity, 37 °C. The tribological evaluation was done using a scratch test, to assess the wear mechanisms and coefficient of friction between stylus and composite material.

2.1 Materials

In this work the resin composite restorative materials used are: a nanohybrid—Composite A and a microfilled—Composite B. Table 1 presents the resin composite restorative materials under study, with details about their matrix composition and reinforcement filler, the latter being subdivided into type, average particle dimension and percentage of fraction in volume and weight.

Sixty parallelepipedic specimens (3 mm \times 6 mm \times 45 mm) were produced for each material using a silicone mould. The mould was placed on a glass slab and filled manually, in one increment, with a slight excess of material and covered in the same manner as the base. Before curing, the composite resin samples were manually compacted applying finger pressure on the upper glass slab, to allow flushing of the excess material and to obtain smoother surfaces. The specimens were then photopolymerized using a halogen light polymerizing unit Bluephase[®] (Ivoclar Vivadent AG, Schaan, Liechtenstein) with a light intensity of 1500 mW/cm² \pm 10 % for 40 s,

Table 2 Groups of the resin composite specimens were divided into and thermocycling conditions: number of cycles, dwell time, bath temperatures and number of samples

Groups	Thermocycling			Number of specimens
	Number of cycles	Dwell time (s)	Bath temperature (°C)	
Control (AC and BC)	0	0	–	20
Thermocycling 1 (AT ₁ and BT ₁)	1500	30	5–55	20
Thermocycling 2 (AT ₂ and BT ₂)	5000	60	5–55	20
	Specimens per resin composite			60

three times on each surface. The curing light intensity was verified with a radiometer Bluephase[®] meter (Ivoclar Vivadent AG, Schaan, Liechtenstein). Subsequently, in order to ensure a complete polymerization, the specimens went into a light/heat furnace Lumamat[®] 100 (Ivoclar Vivadent AG, Schaan, Liechtenstein).

The specimens were manually polished with several Silicon Carbide abrasive paper from grit 320 up to 2500 under continuous water cooling, until minimum permissible roughness was achieved, so that the mechanical properties could be tested. This task was done using a machine LaboPol-5 (Struers, Ballerup, Denmark). When passing from one paper to the other, the specimens were turned approximately 90°, to eliminate the marks created by the previous paper. Subsequently, an ultrasound was passed where the impurities were removed and, to finish, the specimens were dried with an air jet and observed for directional marks on the surface, with an optical microscope.

2.1.1 Thermocycling

Each material's specimens were divided into three groups: a control group, not subjected to aging, and two thermocycled groups. The thermocycled specimens were immersed in baths at the same temperatures but with a different number of cycles and dwell times. Table 2 shows the three groups into which specimens were divided, in which A stands for Composite A, B for Composite B, C for control and T₁ and T₂ for thermocycling 1 and 2, respectively. The thermocycling equipment allows to configure: baths temperature in Celsius degrees, bath dwell time in seconds and number of cycles.

2.2 Experimental procedures

2.2.1 Mechanical characterization

2.2.1.1 Surface roughness Roughness measurements were performed according to the standard ISO 4288 [24]. The measuring apparatus was a mechanical roughness tester, Mitutoyo SurfTest SJ 500P (Mitutoyo Co., Kawasaki, Japan). The monitored parameters are presented in Table 3; R_a , R_z , R_q

Table 3 Monitored roughness parameters

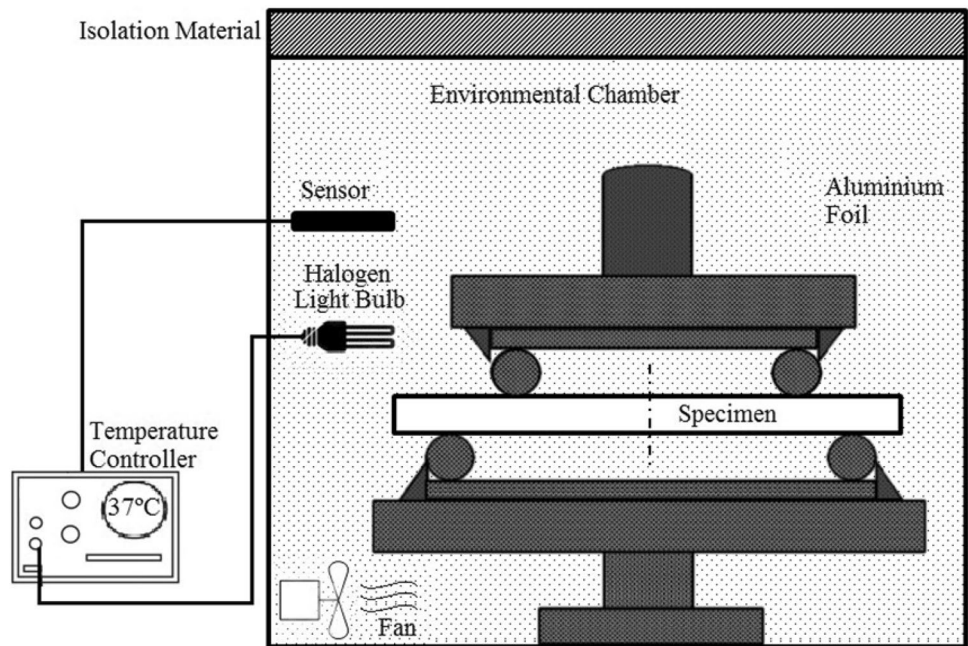
Roughness parameters	
R_a	Average surface roughness
R_q	Root mean square roughness
R_z	Mean roughness depth
R_{sk}	Roughness skewness

and R_{sk} . R_a and R_q arithmetic average and root mean square, respectively, were selected due to their large use and permit to compare sample roughness in what concerns their esthetic aspects. R_z average distance between the highest peak and lowest valley in each sampling length enables to have an idea of the profile total high. The skewness parameter, R_{sk} , is indicated to relate the surface load capability and therefore was selected to evaluate the materials in the study. Roughness measurements were made in all specimens, and five measurements were performed on each specimen, evenly distributed along the surface and perpendicular to the previous one, to minimize the influence of directionality.

The mean dimensions (length, width, thickness) were measured ten times in each direction, for each specimen, using a digital calliper (Mitutoyo Co., Kawasaki, Japan). Each specimen was weighed on a precision scale (A&D, Tokyo, Japan). The specimen geometry used to determine the mechanical properties was a parallelepiped with nominal dimensions of 45 mm long, 6 mm wide and 3 mm thick. All the mechanical tests were made at the controlled temperature of 37 °C.

2.2.1.2 Dynamic test The elastic modulus was measured by the impulse excitation technique as described by Braem et al. [25] and according to the standard ASTM C1259-14 [26]. Before testing, the specimens were heated in an oven, model Digiheat (Selecta, Barcelona, Spain), at 40 °C for 1 h. Each specimen, after being removed from the oven and a temperature of 37 °C was attained, was set in free flexural vibration by a light mechanical impulse. The fundamental frequency of the first flexural vibration mode was determined analyzing the vibrational response by Fast Fourier Transform. Five vibrational signals per specimen were considered in the determination of the elastic modulus.

Fig. 1 Environmental chamber used in bending tests



The elastic modulus obtained through this test will be known as dynamic elastic modulus (E_d) and was calculated as a function of the frequency of the first flexural vibration mode using Eq. (1);

$$E_d = 0.9465 \left(\frac{mf_i^2}{d} \right) \left(\frac{l^3}{t^3} \right) T_1 \quad (1)$$

where l , d and t are, respectively, the length, width and thickness of the bar, m is the mass and f_i is the fundamental frequency of the first flexural vibration mode. According to the ASTM standard, T_1 is a correction factor to take into account the finite dimensions of the specimen. For the calculation of T_1 , a constant Poisson ratio of 0.3 was assumed.

2.2.1.3 Bending test A bending test was carried out by four-point-flexure tests performed according to the standard ASTM C1161-13 [27]. An environmental chamber (Fig. 1) was made to allow testing at the desired temperature (37 ± 2 °C). Resin samples were tested with a Shimadzu Autograph AG-X-5kN Universal Testing Machine (Shimadzu, Kyoto, Japan) with a crosshead speed of 0.5 mm/min using a support lower span of 40 mm and an upper loading span of 20 mm.

In order to determine the static elastic modulus (E_S) the evolution of flexural stress versus crosshead displacement was plotted. In the initial linear part of the curve, the slope represents the resistance to deformation of the material, so is a measure of the static elastic modulus (E_S). The use of Eqs. (2) and (3) allows to determine the static elastic modulus (E_S) and the flexural strength (S), respectively. The work-of-fracture (WOF) was calculated by numerical

integration as the area below the flexural curve that can be used as a comparative value of the toughness. The work-of-fracture (WOF) corresponds to the area below the flexural strength curve and was calculated by numerical integration. It can be used as a comparative value of the toughness.

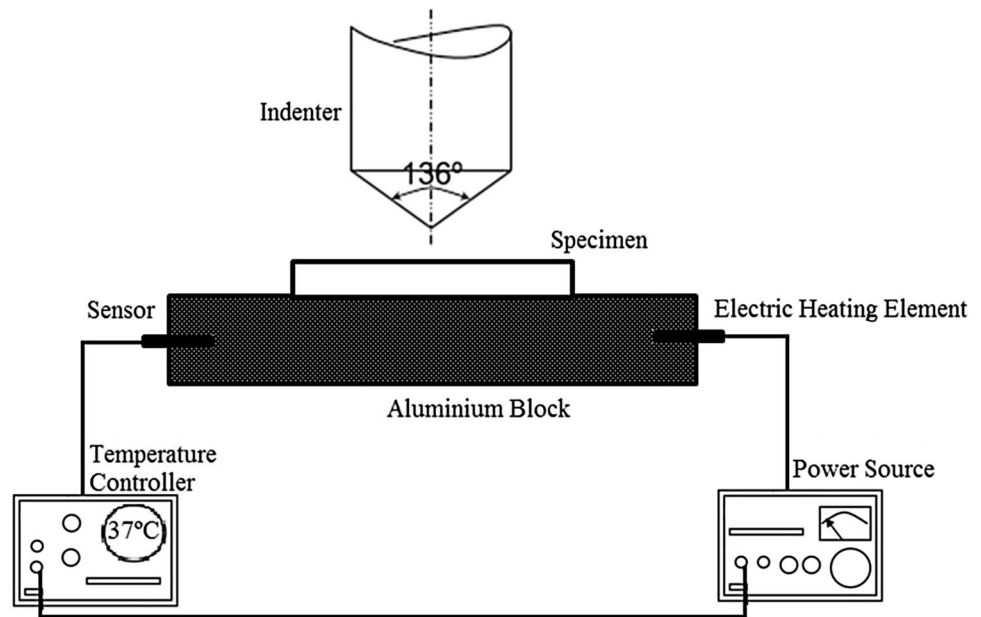
$$E_s = \left(\frac{P}{\delta} \right) \frac{L^3}{8dt^3} \quad (2)$$

$$S = \frac{PL^3}{4dt^2} \quad (3)$$

where P/δ is the slope of the linear part of the load–displacement curve (in N/mm), L is the outer span, d and t are, respectively, the width and the thickness of the specimen (in mm).

2.2.1.4 Hardness To determine the hardness, a Vickers micro-indentation test was carried out, using Struers Duramin (Struers, Ballerup, Denmark) testing equipment, according to the standard ASTM E384-10 [28]. The test temperature was controlled using a specimen base holder shown in Fig. 2. An electric heating element, placed inside an aluminum block, was connected to a power source, heating the aluminum block which, in turn, heated the specimen. Inside the aluminum block, other than the element, there was also a sensor, connected to a temperature controller that, depending on the temperature of the block, turns the power source on or off, maintaining the temperature inside the desired range (37 ± 3 °C). A thermal conducting paste, manufactured by Fisher Elektronik, was smeared on the base of the specimen, in order to increase the rate of heat transfer from

Fig. 2 Assembly used to assess the specimens micro-hardness



the block to the specimen. A load of 1.962 newtons (N) was applied for a period of 40 s; ten indentations were made on the surface of each specimen.

2.2.2 Tribological characterization—scratch test

To determine the coefficient of friction, a scratch test was carried out using a four-axis CNC machine according to the standard ASTM G 171-13 [29]. A stylus made from tungsten carbide, with a rounded tip, 50 μm and conic shape, 60°, was drawn horizontally across the specimens at a constant speed of 0.5 mm/s, with the load increasing linearly over time from 0 to 10 N, producing 5 mm long scratches. The normal and tangential loads were measured through a three-way load cell connected to the specimen bearer. Systematic SEM observations of the specimen's surface were made using a Philips XL30 (Philips, Eindhoven, Netherlands). All the tested specimens were sputter-coated with gold to allow a better observation. The images were attained with secondary and backscattered electrons to make it possible to see the dimension and distribution of the particles and identify the failure mechanisms that occurred in the tests.

3 Results and discussion

A preliminary study was made after the first thermocycled groups (T_1) were produced. Because the effect of thermocycling on the mechanical properties was very small, the heat transfer rate from the water baths to the specimen of resin composite material was studied by finite element method (FEM). The finite element

analysis (FEA) was done using MSC Software's Marc and Mentat (2013); the specimens mesh was done using a linear isoparametric element. The thermal analysis was done considering convective heat transfer in transient regime. The specimen's FEA was executed considering no constriction, the boundary conditions. Three fluid media were considered: distilled water at 5 °C, air at room temperature 20 °C) and distilled water at 55 °C. The parameters used were: $c_p = 837,36 \text{ J/kg K}$, $h = 100 \text{ W/m}^2 \text{ k}$, $k = 1, 2 \text{ W/m K}$ and $\rho = 2000 \text{ kg/m}^3$, where c_p is the heat capacity at constant pressure, h is the heat transfer coefficient, k is the thermal conductivity and ρ is the density. The values used were collected from the literature [30].

From the FEM analysis, it was possible to determine the temperature distribution as shown in Fig. 3. The specimen heats up faster at the edges than at the centre of the specimen, this is due to the larger ratio surface/volume of the specimen's edge in contact with the fluid. Observing Fig. 3, it is possible to note that the temperature rises more slowly in the centre of the specimen. For this FEM analysis, it was considered that the specimen started the cycle at room temperature, 20 °C, in order to simulate the first thermal cycle of the specimens in the baths.

Figure 4 shows that the superficial temperature of the specimen only reaches the temperature of the bath after approximately 50 s of immersion. It is logical to assume that, considering a dwell time inferior to 50 s, not all the parts of the specimen will reach the bath's temperature.

To test the hypothesis that the first thermocycling (T_1), in which the specimens were subjected to 1500 thermal cycles with a dwell time of the specimens in the baths of 30 s, would not be enough to affect the extensive properties

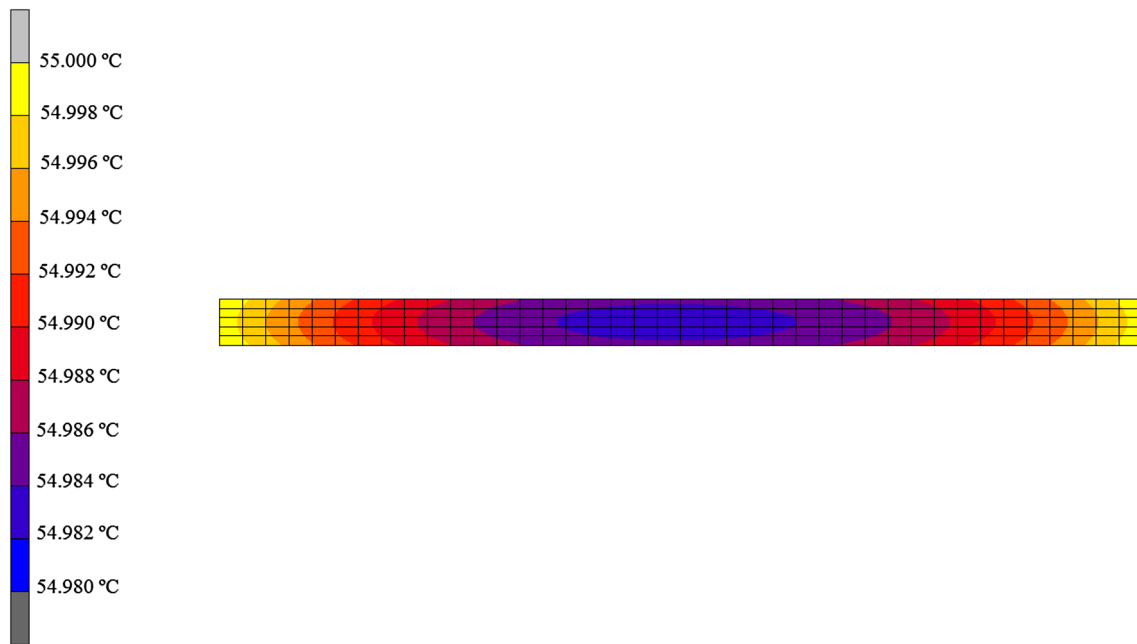


Fig. 3 Middle centre point temperature of a specimen exposed to a water bath at the temperature of 55 °C for 60 s

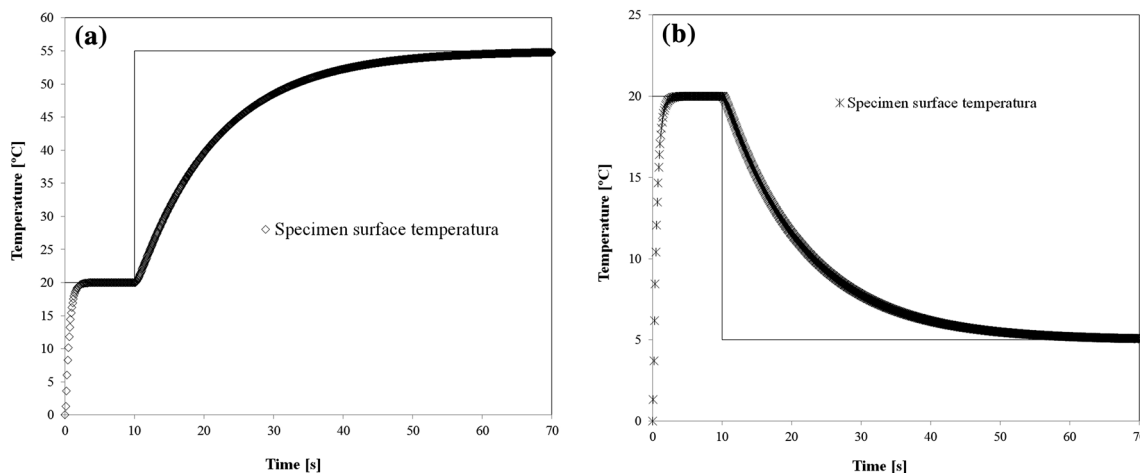


Fig. 4 Middle centre point temperature of a specimen in relation to the time it is exposed to the water baths at: **a** 5 °C, and **b** 55 °C

of the composites in study, a decision was made to process 20 more specimens, and subject them to a more aggressive thermocycling (T_2). These new specimen groups were subjected to 5000 thermal cycles with a dwell time of 60 s for the specimens in the baths, to make sure that the whole volume specimen would be affected.

3.1 Surface roughness

The values obtained for the surface roughness for the different groups of both studied materials are presented in Table 4.

The only parameter that varies significantly with thermocycling is the skewness (R_{sk}), which for Composite B decreased 34 % for BT_1 and increased 57 % for BT_2 . For Composite A, the skewness increased 30 % for AT_1 and 67 % for AT_2 . A negative value of R_{sk} indicates that the surface is made up of valleys, whereas a surface with a positive skewness is said to contain mainly peaks and asperities. Therefore, the general observed trend of an increase of the R_{sk} values was correlated to a decrease of the surficial pores by a swelling effect induced by the thermocycling.

Tuncer et al. [31] only studied the arithmetic average R_a of Composite A, which was very similar to the one obtained

Table 4 Comparison between the roughness parameter average values and respective standard deviations (SD) obtained for Composite A and Composite B control and thermocycled specimen groups

Roughness parameter	Composite A			Composite B		
	AC (SD)	AT ₁ (SD)	AT ₂ (SD)	BC (SD)	BT ₁ (SD)	BT ₂ (SD)
R_a	0.14 (0.04)	0.12 (0.01)	0.15 (0.07)	0.14 (0.06)	0.16 (0.08)	0.17 (0.14)
R_q	0.19 (0.05)	0.16 (0.02)	0.20 (0.09)	0.21 (0.09)	0.27 (0.13)	0.24 (0.06)
R_z	1.47 (0.34)	1.26 (0.19)	1.46 (0.50)	1.73 (0.84)	2.01 (0.60)	1.98 (0.51)
R_{sk}	-1.18 (0.71)	-0.83 (0.56)	-0.39 (0.34)	-1.86 (0.80)	-2.49 (1.34)	-0.79 (0.81)

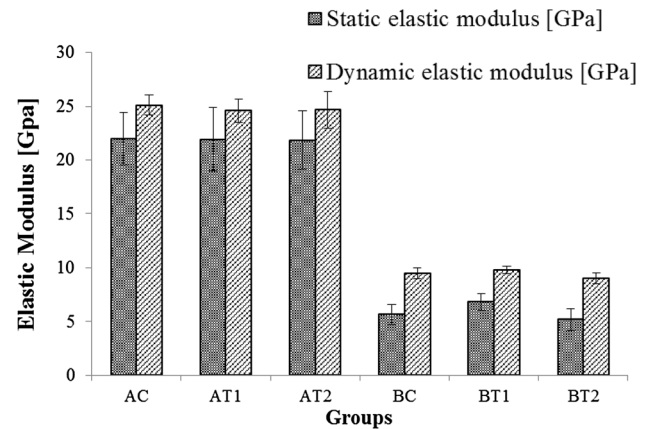
in this study, and concluded that this parameter was not influenced by thermocycling (10,000 cycles between water baths at the temperature of 5 and 55 °C, with a dwell time of 30 s).

3.2 Impulse excitation of vibration

The elastic modulus of the composites under study was measured, using both dynamic and static tests. Hereinafter, the elastic modulus obtained with this test will be known as dynamic elastic modulus.

The dynamic elastic modulus (GPa) of both composites was not significantly affected by thermocycling (Fig. 5). Comparing the values of Composite A and Composite B, it is possible to observe that the dynamic elastic modulus of Composite B is nearly three times lower than that of Composite A. These results mean that, when subjected to the same load, a specimen of Composite B will deform more elastically than a specimen of Composite A. Many researchers have shown that this property is highly dependent on the filler volume fraction, increasing when the filler volume fraction in the matrix of the composite is increased [2, 32, 33]. Composite A contains a much higher volume fraction of inorganic filler particles than Composite B, which explains why it has a much higher elastic modulus.

As can be seen in Fig. 5, the static elastic modulus of Composite A was not affected by the thermocycling aging process, while the dynamic modulus decreased 2 % for AT₁ and 4 % for AT₂. These differences, observed especially on the dynamic modulus, should be correlated to the variation of the viscoelastic behavior of the matrix induced by the thermocycling. On the other hand, the elastic modulus assessed statically for Composite B varies with thermocycling; an increase was noticed for the static elastic modulus of group BT₁, which was 1.2 GPa higher than the static elastic modulus obtained for BC (5.6 GPa) and corresponds to an increase of 22.3 %. This variation could be due to an evolution of the cross-link polymerization of the matrix along the thermocycling, while a decrease of 14.3 % was observed for the static elastic modulus after the BT₂ thermocycling, which was much more aggressive inducing a reduction in rigidity by damage of the matrix or a

**Fig. 5** Comparison between the average values and respective standard deviations obtained for the static and dynamic elastic modulus of Composite A and Composite B control and thermocycled specimen groups

weakness effect on the interface particle–matrix. The variation noticed for the dynamic elastic modulus of Composite B was very small, which can be explained by the fact that the dynamic test induced very small deformations which are less sensitive to the damage in the interface particle–matrix. From Fig. 5, it is noticeable that the dynamic elastic modulus is always greater than the static elastic modulus. The viscoelastic behavior of the resin matrix makes these materials highly dependent on the deformation rate. If the rate of deflection of the specimen was increased during the bending test, the value obtained statically would tend to the value obtained dynamically [34].

The modulus of elasticity of Composite A, measured both dynamically and statically, is always superior to that of Composite B and closer to that of dentin (≈ 19 GPa [35]), which means that the restoration and the dentin will deform in a similar way under load. The modulus of elasticity of Composite A was also measured by other researchers: El-Safty et al. [36] obtained an elastic modulus of 24.1 GPa for Composite A by nano-indentation, which is between the values obtained for the static and dynamic elastic modulus obtained in this study. Belli et al. [37] reported an elastic modulus of 14.6 GPa, obtained by three-point bending.

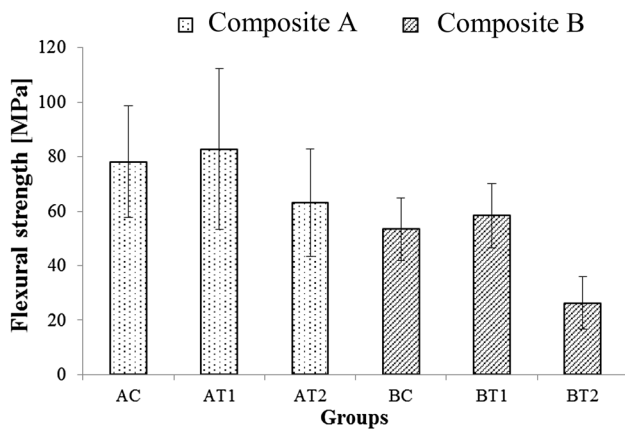


Fig. 6 Comparison of the average values and respective standard deviations obtained for the flexural strength of Composite A and Composite B control and thermocycled specimen groups

3.3 Four-point bending

This test was used to obtain the static elastic modulus, presented in Fig. 5, the flexural strength (MPa), and the work-of-fracture, WOF (J/m^2), of the composites under study.

In Fig. 6, the variations on flexural strength are shown for both materials and for all considered groups. The first thermocycling condition (T_1) caused an increase in the flexural strength of Composite B (14.9 %). However, the second, more aggressive, thermocycling condition (T_2) brought about a pronounced reduction of this property (53.1 %). For Composite A, the flexural strength of AT_1 was nearly equal to that of group AC, but group AT_2 suffered a significant reduction (19.1 %). In this study, the flexural strength obtained for the three groups of Composite B was far from the minimum of 80 MPa required by ISO 4049 [38] for posterior dental restorative materials, and its use in posterior regions of the mouth is not advisable. Although by a very short value, Composite A also missed the imposed condition of 80 MPa required by ISO 4049 [38] (both groups AC and AT_1 , with 78.1 and 79.4 MPa, respectively).

The WOF of Composite B ($2459.3 J/m^2$) was initially higher than the WOF of Composite A ($1435.9 J/m^2$). Composite A has a higher fraction of inorganic reinforcement particles and hence has a higher elastic modulus, which makes it deform less when subjected to a load. Furthermore, the polymer nature of the matrix is different for the two composites and in general lower rigidity and higher deformation is expected for UDMA [39]. The deformation at fracture for a specimen of Composite B is greater, which results in a larger area below the stress–strain curve and, consequently, a greater WOF. This result means that, although more force is necessary to fracture a specimen of Composite A, it will deform less upon fracture than a

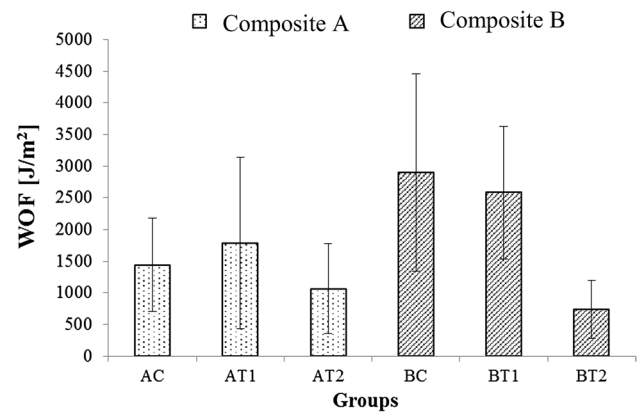


Fig. 7 Comparison of the WOF average values and respective standard deviations obtained for Composite A and Composite B control and thermocycled specimen groups

specimen of Composite B. In both T_1 groups, a slight increase in WOF was noticed, for both materials. However, due to the high standard deviations, it was concluded that this increase was not significant. The WOF diminishes quite a lot for AT_2 (25.8 %) and especially for BT_2 (73.2 %).

The higher values of WOF of Composite B are reported by several authors. Asmussen and Peutzfeldt [40] and Sideridou et al. [41] report that in copolymers bis-GMA/UDMA, the tenacity capabilities increase with the content of UDMA [39, 40]. Ruyter and Øysæd [41] indicate that a possible explanation for this finding may be found in the rather flexible nature of UDMA, which has been observed with some urethane polymers. Peutzfeldt and Asmussen [42] noted that some compositions of relatively high content of UDMA are at the same time rather flexible and strong. Such materials are by definition characterized by a considerable modulus of resilience or toughness [43].

As can be seen in Figs. 5, 6 and 7, the standard deviations of the properties obtained through this test are very high, which means that the results varied a lot from specimen to specimen. The four-point bending test is highly dependent on the quality of the specimens since the load applied by the cylindrical rolls is applied on a wide area and the presence of superficial defects, such as pores, may induce the premature fracture of the specimen. Nevertheless, composite materials in general are characterized by a high variability of their properties.

In general, Composite B seems to be more affected by thermocycling conditions than Composite A. Since Composite B has a lower filler volume fraction, it has higher resin content, which is precisely the main factor responsible for the water sorption in aqueous environments. The monomers that constitute the matrix of both composites may have influenced these results. According to Sideridou

et al. [8], a BisGMA-based composite has more stable mechanical properties in aqueous environments than a UDMA-based composite. Other researchers observed that UDMA-based composites more easily experience a softening in aqueous environments than BisGMA-based composites [44, 45].

The increase in static elastic modulus and flexural strength of group BT₁ was unexpected and hard to explain. Besides these two parameters, the skewness of group BT₁ also decreased. It actually seems that the first thermocycling condition (T₁) improved the mechanical properties of Composite B. It is well established that the exposure of resin composites to aqueous environments lowers their mechanical properties [46]. However, some studies demonstrate that water sorption during aging may cause a plasticizing of the tough but slightly brittle resin matrix, making resin composites more flexible, which causes an apparent increase in mechanical properties [47, 48]. However, all results lead us to conclude that in the case of Composite B, the mild thermocycling condition T₁ seems complete the cross-linking polymerization which could explain both the increase of the number of pores, hence the reduction of the roughness skewness, and the increase of the mechanical properties. While for the more aggressive condition, the degradation of the matrix was superposed to this favorable effect.

The degradation observed for groups AT₂ and BT₂ may be explained by the entry of water in the material, which breaks the link between the organic matrix and the inorganic filler particles [8, 49, 50]. The failure of the coupling agent, by hydrolysis, promotes the degradation of the matrix and the elution of fillers from the matrix, originating pores, hence diminishing the material's flexural strength and toughness. The huge degradation in flexural strength and work of fracture observed for group BT₂ may signify that a generalized failure of the UDMA matrix occurred, caused by water sorption [8, 51].

3.4 Micro-hardness

The micro-hardness obtained for Composite A was more than three times greater than that of Composite B, Fig. 8. The hardness of both materials does not seem to be significantly affected by thermocycling conditions since the largest reduction, percentage-wise, was observed for BT₂, which lowered by 7.5 %.

It is well established in the literature that hardness raises with the increase in filler volume fraction [2, 33]. As Composite A possesses a filler volume fraction much superior to Composite B, it was expected that its hardness would be greater than that of Composite B. The micro-hardness of enamel has been measured at around 4000 MPa and dentin

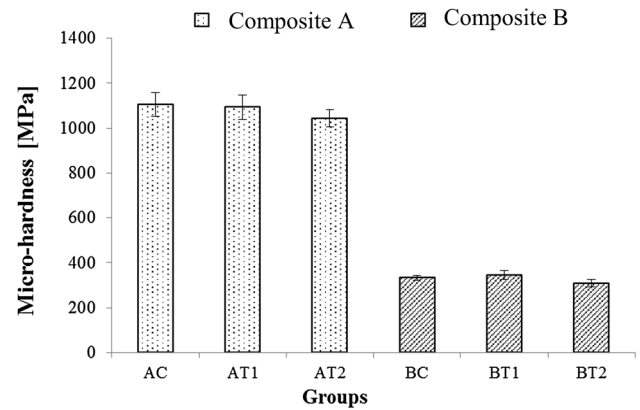


Fig. 8 Comparison of the average values and respective standard deviations obtained for the micro-hardness of Composite A and Composite B control and thermocycled specimen groups

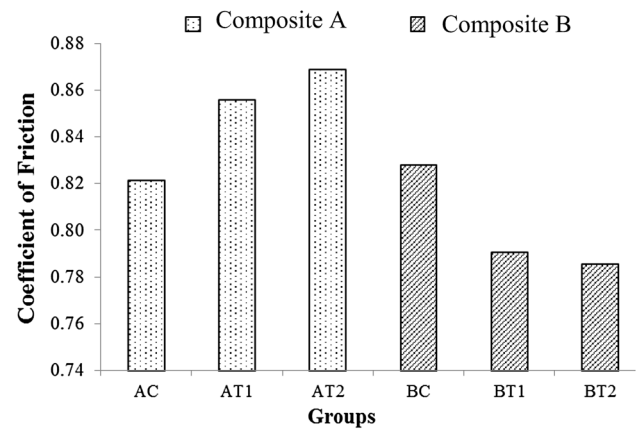


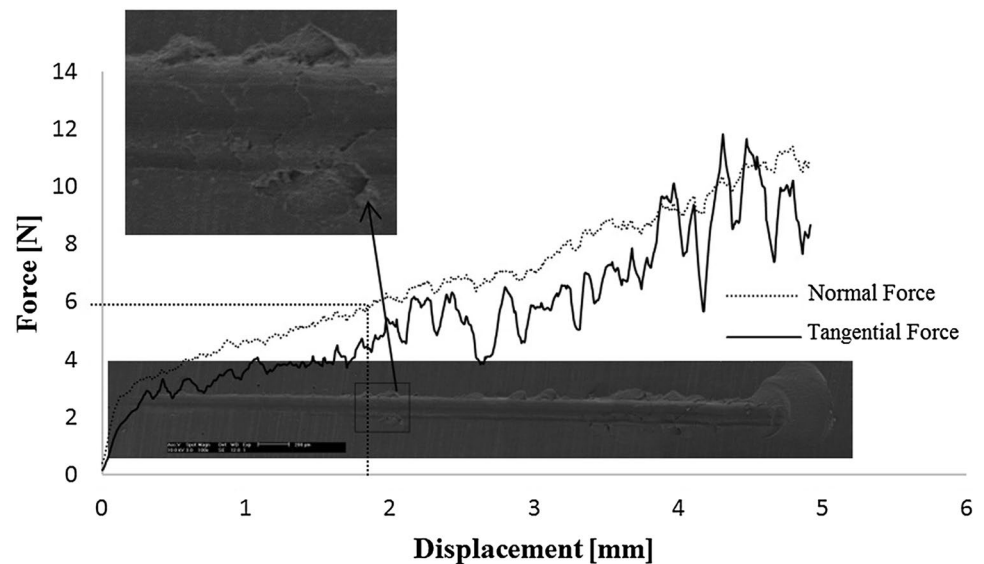
Fig. 9 Comparison between the coefficient of friction of Composite A and Composite B control and thermocycled specimen group

at around 1000 MPa [52]. By these results, only Composite A shows micro-hardness close to that of dentin (see Fig. 8).

Other researchers studied the hardness of Composite A. Tuncer et al. [31] studied the micro-hardness of Composite A after 10,000 thermal cycles between baths at 5 and 55 °C, with a dwell time of 30 s and obtained a micro-hardness of 1430 MPa (146 Vickers) for the control group and a micro-hardness of 1180 MPa (129 Vickers) after thermocycling. El-Safty et al. [36] reported a nano-hardness of 1600 MPa for Composite A. Alshali et al. [53] studied the post-irradiation hardness development of Composite A and found that the maximum hardness was 950 MPa (97.5 Vickers), for 24-h post-curing.

According to Rahim et al. [54], composite degradation can be induced by two mechanisms. The first mechanism is due to the diffusion of water molecules into the polymer network; water molecules occupy the free volume between

Fig. 10 Wear scar obtained by SEM analysis for a specimen of Composite A, group AC, juxtaposition with normal and tangential loads



polymer chains and microvoids, causing plasticization and swelling of the polymer matrix and also initiate the chain's scission causing monomer elution [55, 56]. The water molecules also tend to degrade the siloxane bonds (bond between silanol groups of the silica surface and the silane coupling agent) via a hydrolysis reaction, causing filler debonding [55]. These occurrences lead to the degradation or softening of resin composites which may diminish some physical and mechanical properties such as hardness, strength and modulus of elasticity [54].

Ferracane [56] affirms that water sorption of polymer composites is also highly dependent upon the chemical structure of the resin monomers. The monomers are hydrophilic in nature due to the presence of polar groups in their structure which tends to be attracted by water molecules to form hydrogen bonding [54]. Nevertheless, the degree of hydrophilicity of monomers varies, depending on the type of functional groups obtained in monomer structure. The hydroxyl group, for instance, present in BisGMA would form a stronger hydrogen bonding with water molecules compared to ether and urethane linkage found in BisEMA and UDMA, respectively [57]. Kalachandra and Turner [58] have shown that water sorption is greater for BisGMA containing higher concentrations of TEGDMA. In the referred study, they compared two composites, one only with UDMA monomer against another which had a combination of BisGMA and other dimethacrylate monomers (TEGDMA, BisEMA and UDMA) and the composited with UDMA monomer registered less water sorption [54].

When comparing hardness and the other material properties tested there is almost no influence of the thermocycling on the materials hardness, this could be explained due to good plastic compression resistance of composites. Since the weakness of the interface matrix particle is one

of the main identified mechanisms of failure induced by water, this effect should play a reduced action in compressive tests.

3.5 Scratch test

Fundamental knowledge about mechanical behavior during scratch tests is not nearly as developed as indentation testing owing to the complex damage mechanisms involved. The first approach to this was towards a parameter quantifying the coefficient of friction (COF) of both materials, Composite A and Composite B.

Regarding COF Composite A specimens groups increased with thermocycling, the COF of Composite B specimens group diminished with increasing thermocycling severity, Fig. 9.

Figures 10, 11, 12, 13, 14 and 15 represent the wear scars left by the stylus on the Composite A and Composite B specimens, respectively. In all figures, the normal and the tangential forces measured by the load cell can be related for the different groups under study to the respective wear scar. By analyzing the wear scars, it is possible to identify the exact location and the respective loads which caused the major local failures. A large fluctuation of the tangential force was noticed in all groups of Composite A due to the presence of many hard filler particles, which increase the resistance to the progress of the stylus, reaching the point where enough local stress propagates a crack which causes an instantaneous drop of the friction force, with the subsequent starting of a new increase.

Heintze et al. [33] observed that highly filled composites provide higher friction, since the asperities of the antagonist material collide with a surface which is rich in hard particles and, therefore, more difficult to plough into. However,

Fig. 11 Wear scar obtained by SEM analysis for a specimen of Composite A, group AT₁, juxtaposition with normal and tangential loads

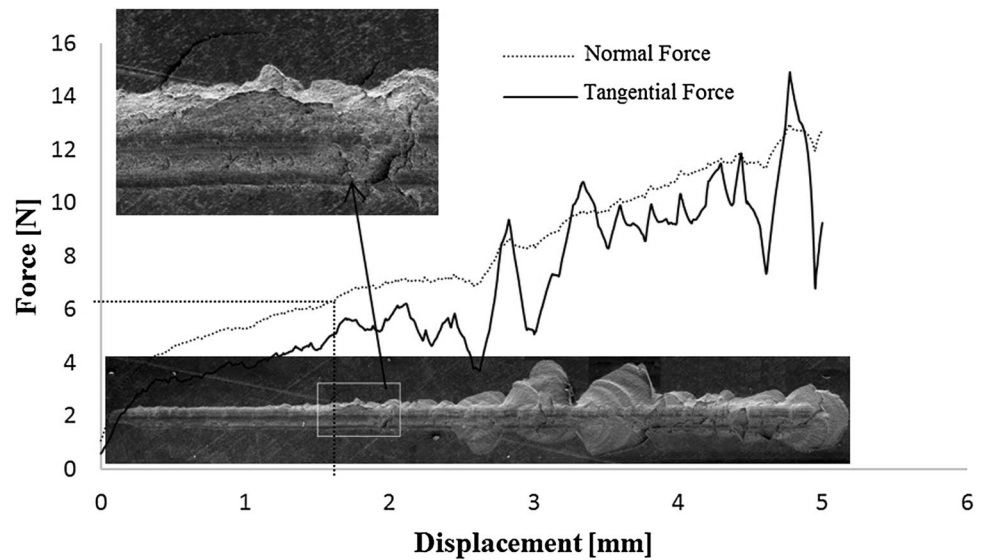
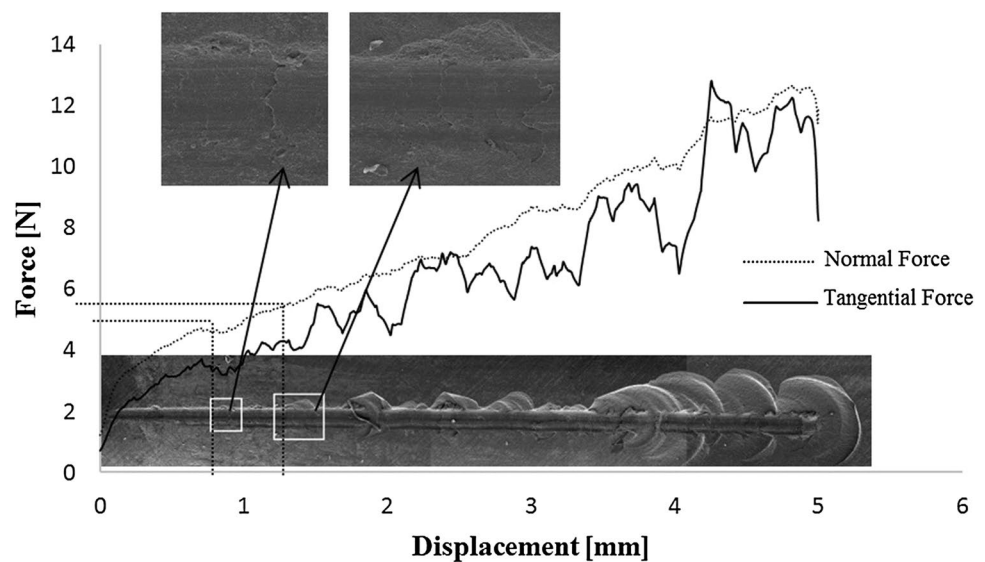


Fig. 12 Wear scar obtained by SEM analysis for a specimen of Composite A, group AT₂, juxtaposition with normal and tangential loads



several researchers noticed that materials with high fracture toughness are more wear resistant [2, 33], and if the filler volume fraction is increased, the toughness of the material diminishes. Larger particles increase the coefficient of friction and, consequently, the contact forces. An increase in the filler size may increase the dimension of the wear debris, because whole reinforce particles may be removed. Regarding scar shape, it is possible to observe an increase in the scar contour with an increase in thermocycling conditions, and it is also possible to find failures for smaller normal loads. These results agree with the reduction of the toughness induced by thermocycling, as observed by the WOF values.

Regarding the behavior of Composite A and considering the control and thermocycled groups, as the tangential load

increases the specific contact stress field is reflected in the material in the form of a compressive area in front of the advancing indenter and of a tensile stress field at its back [59]. When the stress overcomes the specific strength of the material, massive delamination phenomena occur, similar to data reported on thermoset and thermoplastic organic coatings [60]. The brittle nature of the delamination phenomenon of the material tested with the sharper indenter is confirmed by the area of damage, more noticeable in groups with thermocycling, and especially for group AT₂. The damage spreads at the sides and ahead of the actual contact between the indenter and the material surface as a result of a brittle spallation phenomenon. The more severe the thermocycling, the more severe the corresponding spallation phenomenon after the progressive load scratch test [61].

Fig. 13 Wear scar obtained by SEM analysis for a specimen of Composite B, group BC, juxtaposition with normal and tangential loads

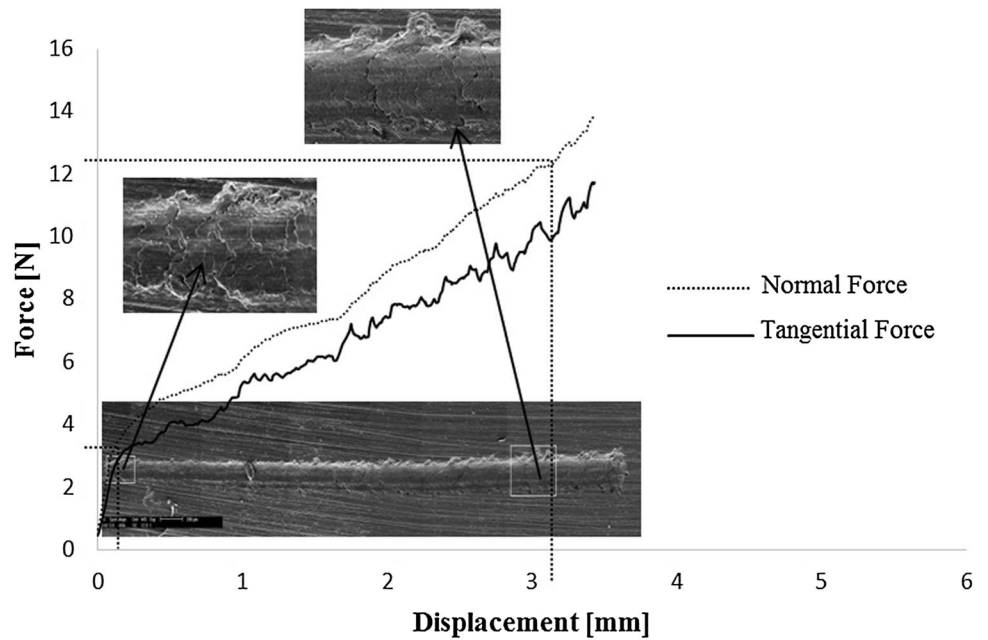
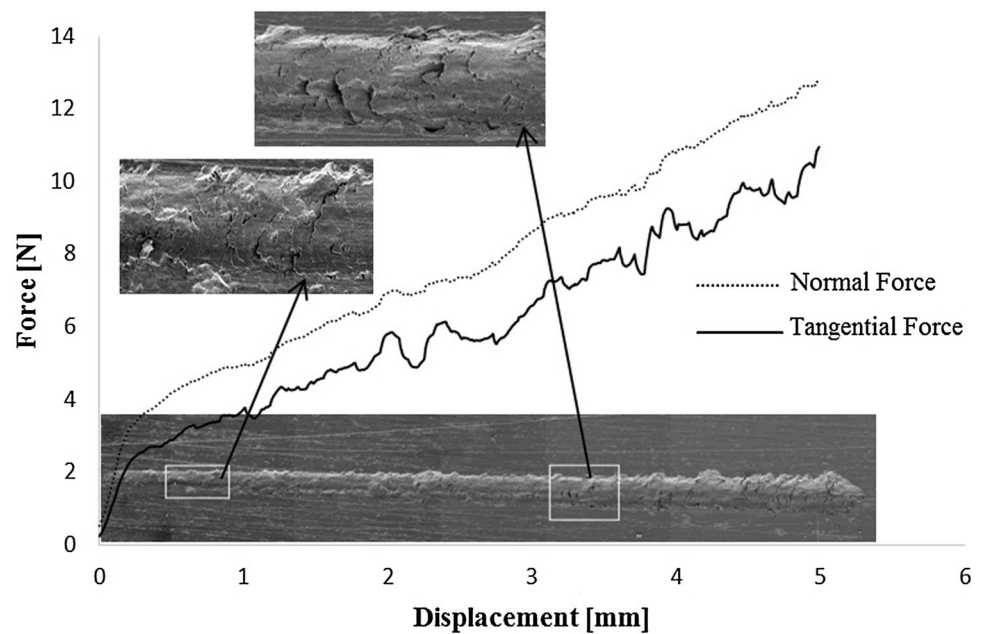


Fig. 14 Wear scar obtained by SEM analysis for a specimen of Composite B, group BT₁, juxtaposition with normal and tangential loads



The main failure mode observed for Composite A is by chipping of composite debris, noticeable on the edges of the scratch, with little plastic deformation along the wear scar. Figures 10, 11 and 12 show that the wear removal by chipping happens at peaks of tangential force. When an increase is accompanied by a sudden and sharp decrease of the tangential force, it is likely that chipping occurred. The compression stresses ahead of the stylus are responsible for the chipping observed in this test. The presence of some large and brittle particles acts as an enabling factor for the

crack propagation. A filler particle of over 5 μm , found on the fracture surface of group AC, is shown in Fig. 16.

For Composite B, which has a lower volume of filler particles and a larger amount of organic matrix than Composite A, the main failure mode obtained by scratch test was micro-cracks on the wear scar, brought about by the plastic deformation caused by the tensile stresses, behind the stylus, Figs. 13, 14 and 15. As Composite B is tougher than Composite A, it dissipates better the stresses applied by the stylus, reducing the quantity of wear debris and increasing

Fig. 15 Wear scar obtained by SEM analysis for a specimen of Composite B, group BT₂, juxtaposition with normal and tangential loads

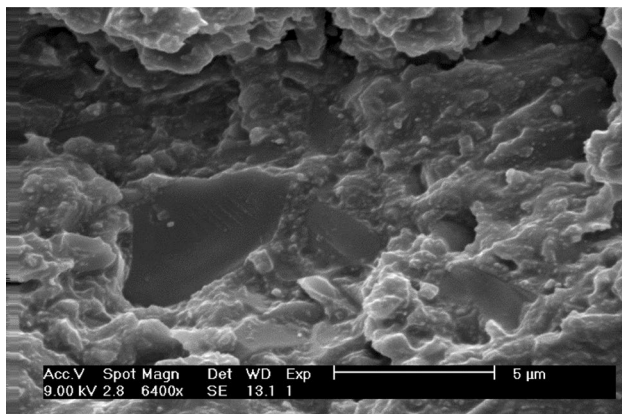
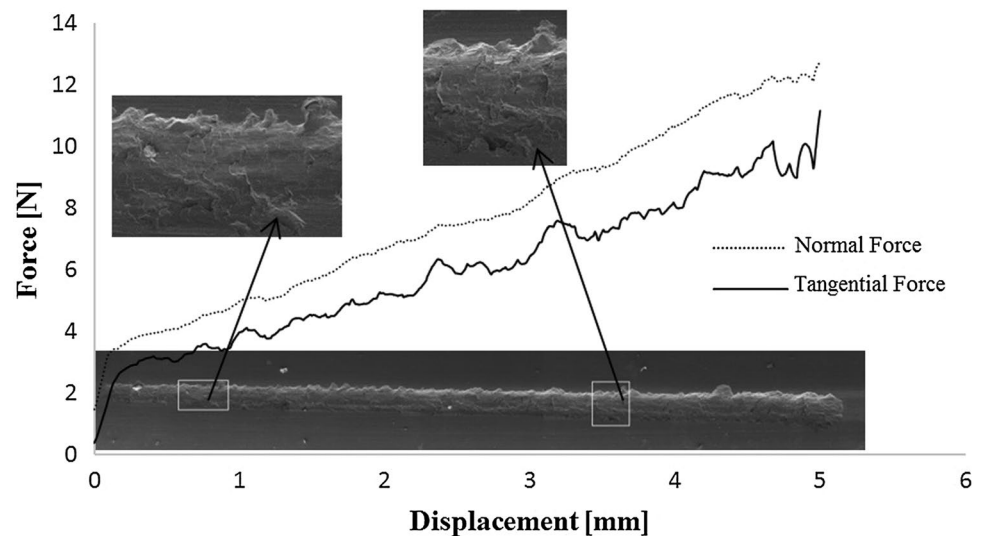


Fig. 16 SEM analysis of a specimen of Composite A, group AC, amplified 6400 times

the plastic deformation. Some chipping was observed in the borders of the wear scar, more notable in group BT₂, Fig. 17. It is hard to qualify the fractures caused by tensile stresses in Composite B, since the scratches are notable perfect at the beginning of the wear scar, in all tested groups. This behavior is also possible to explain based on the nature of Composite B with a UDMA matrix, which is a softer material and also due to the lower inorganic filling percentage when compared to Composite A. The difference in scratch test is also confirmed by the results in microhardness test values, with Composite A's average values more than three times greater than that of Composite B.

Several researchers [62–64] found that the lower the skewness, the lower the contact area and, consequently, the lower the coefficient of friction. Țălu et al. [65] state that negative R_{sk} shows the positive load-resistance ability of the surface of dental composites, which would have

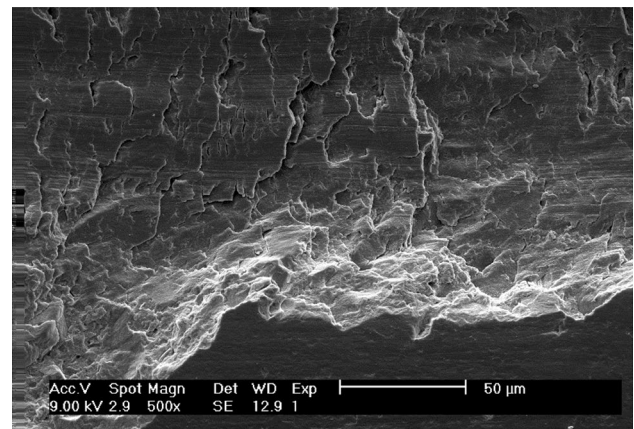


Fig. 17 Wear scar obtained by SEM analysis for a specimen of Composite B, BT₂ group, augmented $\times 500$. There is plastic deformation at the center of the wear scar and localized chipping on scratch borders

a relatively stable wear rate during function. The larger amount of valleys in the composites would allow them to retain the saliva which would have a role of a lubricant in this specific naturally engineered environment. In the present study, a negative skewness should not have any beneficial influence because the dry sliding condition was used, and considering the brittle nature of the composites any surface asperity would have a detrimental effect both for valleys and peaks. The variation of the COF is much more related to mechanical resistance. In the case of the Composite B, the decrease of the mechanical resistance with thermocycling explains the rise in friction. The UDMA matrix suffered a general degradation due to the sorption of water, reducing its capacity to withstand the advance of the stylus and, consequently, diminishing the coefficient of

friction. While for the case of Composite A, the spalling of the material ahead of the stylus generates a rough surface which induces high friction.

Regarding the tribological evaluation, the test selected was the scratch test, which is a load-scanning test that allows a change in the applied load and, consequently, the friction force throughout the test, as well as correlating these parameters with stress distribution and contact morphology. Palaniappan et al. [66] observed a very high correlation between in vitro scratch tests and clinical contact-free occlusal area wear and concluded that scratch tests could roughly categorize a new material as to whether it will probably exhibit a high or low wear rate. This simple and quick test can, therefore, be a great alternative to other more time-consuming wear tests in order to compare and rank wear performance of novel resin composites. This in vitro scratch test appears to potentially provide a rapid way of screening materials to assess expected clinical wear performance.

To summarize the limitation of the present study, the conditions expressed in standard ISO 11405 [1] are not adequate to infer a proper thermocycling effect on restorative materials. The tests evaluations vary from author to author and, therefore, it is difficult to compare results from similar works. Although the experimental procedures are robust and it incorporates a multi-parametric analysis, the number of material tested is reduced. A higher number of materials would definitely evaluate the thermocycling effect on restorative materials. Regarding future recommendations, it would be of great importance to increase the number of cycles regarding the aging, quantify the scratch test and validate the scratch tests with some reciprocating wear tests.

4 Conclusions

In the present study, the effect of thermocycling on the mechanical and tribological properties of two indirect restoration dental composite materials, Composite B and Composite A, currently marketed, was evaluated.

Both numerical finite element analysis and the experimental results lead us to conclude that the number of cycles and dwell times of the specimens in the baths imposed by standard ISO 11405 [1] for thermocycling studies are not sufficient to significantly alter the mechanical properties of modern resin composites. A larger number of thermal cycles and a substantial increase of the dwell time may be representative of the aging that restorative materials are subjected to in the oral cavity.

Regarding the mechanical properties, it could be concluded that:

- Comparing the two tested composites, Composite A has much better mechanical properties in general, due to the difference in the nature of the polymeric matrix and the content of inorganic particles;
- From a general viewpoint on the effect of thermocycling in the reduction of mechanical properties:
 - the hardness was not affected for both composites;
 - the elastic modulus of Composite A was slightly reduced, while Composite B displayed a drop in elastic modulus after thermocycling;
 - in general, Composite B was more affected by thermocycling.

With regard to the tribological evaluation, it could be concluded that:

- The coefficient of friction of Composite A increased with thermocycling, while the coefficient of friction of Composite B decreased with thermocycling. The different behaviors were dependent on the failure mechanisms displayed by the two materials tested.
- The wear mechanisms predominant in Composite A are spallation and chipping. For Composite B, the main wear mechanism observed was plastic deformation, with chipping of material restricted to the borders of the wear scar.

References

1. ISO/TS 11405:2015 Dental materials—testing of adhesion to tooth structure. International Organization for Standardization, Geneva, Switzerland. <https://www.iso.org/obp/ui/#iso:std:iso:ts:11405:ed-3:v1:en>
2. Antunes PV, Ramalho A, Carrilho EVP (2014) Mechanical and wear behaviors of nano and microfilled polymeric composite: effect of filler fraction and size. *Mater Des* 61:50–60
3. Asmussen E, Peutzfeldt A (1998) Influence of UEDMA, Bis-GMA and TEGDMA on selected mechanical properties of experimental resin composites. *Dent Mater* 14:51–56
4. Ru S, Raab WH, Janda R (2007) Polymerization shrinkage and hygroscopic expansion of contemporary posterior resin-based filling materials—A comparative study. *J Dent* 35:806–813
5. Amirouche-Korichi A, Mouzali M, Watts DC (2009) Effects of monomer ratios and highly radiopaque fillers on degree of conversion and shrinkage-strain of dental resin composites. *Dent Mater* 25:1411–1418
6. Amirouche-Korichi A, Mouzali M, Watts DC (2012) Shrinkage strain—rates study of dental composites based on (Bis-GMA/TEGDMA) monomers. *Arab J Chem*. doi:10.1016/j.arabjc.2012.07.021
7. Indrani DJ, Cooks WD, Televantos F, Martin J, Harcourt JK (1995) Fracture toughness of water-aged resin composite restorative materials. *Dent Mater* 11:201–207
8. Sideridou ID, Karabela MM, Bikiaris DN (2007) Aging studies of light cured dimethacrylate-based dental resins and a resin composite in water or ethanol/water. *Dent Mater* 23:1142–1149

9. Mesquita RV, Geis-Gerstorfer J (2008) Influence of temperature on the visco-elastic properties of direct and indirect dental composite resins. *Dent Mater* 24:623–632
10. Ramalho A, Braga de Carvalho MD, Antunes PV (2013) Effects of temperature on mechanical and tribological properties of dental restorative composite materials. *Tribol Int* 63:186–195
11. Musanje L, Darvell BW (2004) Effects of strain rate and temperature on the mechanical properties of resin composites. *Dent Mater* 20:750–765
12. Gale MS, Darvell BW (1999) Thermal cycling procedures for laboratory testing of dental restorations. *J Dent* 27:89–99
13. Göhring TN, Gallo L, Lüthy H (2005) Effect of water storage, thermocycling, the incorporation and site of placement of glass-fibers on the flexural strength of veneering composite. *Dent Mater* 21:761–772
14. Meriç G, Ruyter IE (2007) Effect of thermal cycling on composites reinforced with two differently sized silica-glass fibers. *Dent Mater* 23:1157–1163
15. Morresi AL, D'Amario M, Capogreco M, Gatto R, Marzo G, D'Arcangelo C, Monaco A (2014) Thermal cycling for restorative materials: does a standardized protocol exist in laboratory testing? A literature review. *J Mech Behav Biomed Mater* 29:295–308
16. Zheng SY, Zheng J, Gao SS, Yu BJ, Yu HY, Qian LM, Zhou ZR (2011) Investigation on the microtribological behaviour of human tooth enamel by nanoscratch. *Wear* 271:2290–2296
17. Palaniappan S, Celis J-P, Meerbeek BV, Peumans M, Lambrechts P (2013) Correlating in vitro scratch test with in vivo contact free occlusal area wear of contemporary dental composites. *Dent Mater* 29(3):259–268
18. Ferreira VR, Sukumaran J, Delgado YP, Staia M, Iost A, Baets PD (2013) Scratch evaluation on a high performance polymer. *Mech Eng Lett* 9:76–84
19. Yamamoto T, Hanabusa M, Momoi Y, Sakaguchi RL (2015) Polymerization stress of dental resin composite continues to develop 12 hours after irradiation. *J Esthet Restor Dent* 27(1):44–54
20. Fugolin APP, Correr-Sobrinho L, Correr AB, Sinhoreti MAC, Guirraldo RD, Consani S (2016) Influence of irradiance on Knoop hardness, degree of conversion, and polymerization shrinkage of nanofilled and microhybrid composite resins. *General Dent* 64:26–31
21. Narene AVK, Veniashok B, Subbiya A, Vivekanandhan P, Sukumaran VG (2014) Polymerisation shrinkage in resin composites—a review. *Middle East J Sci Res* 21:107–112
22. Yang S, Choi J, Cho M (2012) Elastic stiffness and filler size effect of covalently grafted nanosilica polyimide composites: molecular dynamics study. *ACS Appl Mater Interfaces* 4:4792–4799
23. Mandikos MN, McGivney GP, Davis E, Bush PJ, Carter JM (2001) A comparison of the wear resistance and hardness of indirect composite Resins. *J Prosthet Dent* 85(4):386–395
24. ISO 4288:1996/Cor.1:1998 (en), Geometrical Product Specifications (GPS)—Surface texture: profile method—rules and procedures for the assessment of surface texture, International Organization for Standardization, Geneva, Switzerland
25. Braem M, Lambrechts P, Doren VVAN, Vanherle G (1986) The impact of composite structure on its elastic response. *J Dent Res* 65:648–653
26. C1259 (2015) Standard test method for dynamic young's modulus, Shear modulus, and poisson's ratio for advanced ceramics by impulse excitation of vibration, Developed by subcommittee: C28.01, Book of standards vol 15.01, American Society for Testing and Materials ASTM C1259
27. C1161 (2013) Standard test method for flexural strength of advanced ceramics at ambient temperature, Developed by subcommittee: C28.01, Book of standards vol 15.01, American Society for Testing and Materials ASTM C1161
28. E384 (2016) Standard test method for microindentation hardness of materials, Developed by subcommittee: E04.05, Book of standards vol 03.01, American Society for Testing and Materials ASTM E384-16
29. G171 (2009) Standard test method for scratch hardness of materials using a diamond stylus, Developed by subcommittee: G02.30, Book of standards vol 03.02, American Society for Testing and Materials ASTM G171-03(2009)e2
30. Stalio E (2002) Direct numerical simulation of heat transfer enhancing surfaces. Doctoral Thesis, pp 75–90
31. Tuncer S, Demirci M, Tiryaki M, Ünlü N, Uysal Ö (2013) The effect of a modeling resin and thermocycling on the surface hardness, roughness, and color of different resin composites. *J Esthet Restor Dent* 25:404–419
32. Beun S, Glorieux T, Devaux J, Vreven J, Leloup G (2013) Characterization of nanofilled compared to universal and microfilled composites. *Dent Mater* 23:51–59
33. Heintze SD, Zellweger G, Zappini G (2007) The relationship between physical parameters and wear of dental composites. *Wear* 263:1138–1146
34. Mesquita RV, Axmann D, Geis-Gerstorfer J (2006) Dynamic visco-elastic properties of dental composite resins. *Dent Mater* 22:258–267
35. Xu HH, Smith DT, Jahanmir S, Romberg E, Kelly JR, Thompson VP, Rekow ED (1998) Indentation damage and mechanical properties of human enamel and dentin". *J Dent Res* 77:472–480
36. El-Safty S, Akhtar R, Silikas N, Watts DC (2012) Nanomechanical properties of dental resin-composites. *Dent Mater* 28:1292–1300
37. Belli R, Petschelt A, Lohbauer U (2014) Are linear elastic material properties relevant predictors of the cyclic fatigue resistance of dental resin composites? *Dent Mater* 30:381–391
38. ISO 4049:2009 (2009) Dentistry—polymer-based restorative materials, ISO/TC 106/SC 1, standard was last reviewed in 2014, International Organization for Standardization, Geneva, Switzerland
39. Asmussen E, Peutzfeldt A (1998) Influence of UDMA, bis-GMA and TEGDMA on selected mechanical properties of experimental resin composites. *Dent Mater* 56:14–51
40. Sideridou ID, Karabela MM, Bikiaris DN (2009) Aging studies of light cured dimethacrylate-based dental resins and a resin composite in water or ethanol/water. *Dent Mater* 23(9):1142–1149
41. Ruyter IE, Øysæd H (1987) Composites for use in posterior teeth: composition and conversion. *J Biomed Mater Res* 21:11–23
42. Peutzfeldt A, Asmussen E (1992) Modulus of resilience as predictor for clinical wear of restorative resins. *Dent Mater* 8:146–148
43. Asmussen E, Peutzfeldt A (1998) Influence of UEDMA Bis-GMA and TEGDMA on selected mechanical properties of experimental resin composites. *Dent Mater* 14(1):51–56
44. Ho CT, Vijayaraghavan TV, Lee SY, Tsai A, Huang HM, Pan LC (2001) Flexural behaviour of post-cured composites at oral-simulating temperatures. *J Oral Rehabil* 28:658–667
45. Kao EC (1989) Influence of food-simulating solvents on resin composites and glass-ionomer restorative cement. *Dent Mater* 5:201–208
46. Ferracane JL, Berge HX, Condon JR (1998) In vitro aging of dental composites in water—effect of degree of conversion, filler volume, and filler-matrix coupling. *J Biomed Mater Res* 42:465–472
47. Ferracane JL, Berge HX (1988) Fracture toughness of experimental dental composites aged in ethanol. *J Dent Res* 74:1418–1423

48. Pilliar RM, Vowles R, Williams DF (1987) The effect of environmental aging on the fracture toughness of dental composites. *J Dent Res* 66:722–726
49. Prakki A, Cilli R, Mondelli RFL, Kalachandra S, Pereira JC (2005) Influence of pH environment on polymer based dental material properties. *J Dent* 33:91–98
50. Ortengren U, Andersson F, Elgh U, Terselius B, Karlsson S (2001) Influence of pH and storage time on the sorption and solubility behaviour of three composite resin materials. *J Dent* 29:35–41
51. Sarkar NK, Karmaker A, Prasad A, Shih F (1999) Simulation of in vivo degradation of dental composites. *J Mater Sci Lett* 18:1749–1752
52. Zaytsev D, Panfilov P (1999) Deformation behavior of human enamel and dentin-enamel junction under compression. *Mater Sci Eng C* 34:15–21
53. Alshali RZ, Salim NA, Satterthwaite JD, Silikas N (2015) Post-irradiation hardness development, chemical softening, and thermal stability of bulk-fill and conventional resin-composites. *J Dent* 43:209–218
54. Rahim TNAT, Mohamad D, Akil HM, Rahman IA (2012) Water sorption characteristics of restorative dental composites immersed in acidic drinks. *Dent Mater* 28(6):e63–e70
55. Ferracane JL (2006) Hygroscopic and hydrolytic effects in dental polymer networks. *Dent Mater* 22(3):211–222
56. Curtis AR, Shortall AC, Marquis PM, Palin WM (2008) Water uptake and strength characteristics of a nanofilled resin-based composite. *J Dent* 36(3):186–193
57. Moraes RR, Sinhoreti MAC, Correr-Sobrinho L, Ogluari FA, Piva E, Petzhold CL (2010) Preparation and evaluation of dental resin luting agents with increasing content of bisphenol-A ethoxylated dimethacrylate. *J Biomater Appl* 24(5):453–473
58. Kalachandra S, Turner DT (1987) Water sorption of polymethacrylate networks: Bis-GMA/TEGDM copolymers. *J Biomed Mater Res* 21(3):329–338
59. Kobrick RL, Klaus DM, Street KW (2011) Standardization of a volumetric displacement measurement for two-body abrasion scratch test data analysis. *Wear* 270(9–10):650–657
60. Jardret V, Morel P (2003) Viscoelastic effects on the scratch resistance of polymers: relationship between mechanical properties and scratch properties at various temperatures. *Prog Org Coat* 48:322–331
61. Barletta M, Gisario A, Trovalusci F, Vesco S (2013) Visual appearance and scratch resistance of high performance thermoset and thermoplastic powder coatings. *Prog Org Coat* 76:244–256
62. Barletta M, Tagliaferri V, Gisario A, Venettacci S (2013) Progressive and constant load scratch testing of single- and multi-layered composite coatings. *Tribol Int* 64:39–52
63. Bastos FS, Oliveira EA, Fonseca LG, Vargas SM, Las Casas EB (2016) A FEM-based study on the influence of skewness and kurtosis surface texture parameters in human dental occlusal contact. *J Comput Appl Math* 295:139–148
64. Sedlaček M, Podgornik B, Vižintin J (2012) Correlation between standard roughness parameters skewness and kurtosis and tribological behaviour of contact surfaces. *Tribol Int* 48:102–112
65. Țălu Ș, Stach S, Lainović T, Vilotić M, Blažić L, Alb SF, Kakaš D (2015) Surface roughness and morphology of dental nanocomposites polished by four different procedures evaluated by a multifractal approach. *Appl Surf Sci* 330:20–29
66. Palaniappan S, Celis J-P, Van Meerbeek B, Peumans M, Lambrechts P (2013) Correlating in vitro scratch test with in vivo contact free occlusal area wear of contemporary dental composites. *Dent Mater* 29:259–268